The Structure of the Proton and HERA

Max Klein

University of Liverpool, Physics Department, Oxford Street, L69 7ZE Liverpool, UK

DOI: http://dx.doi.org/10.3204/DESY-PROC-2009-03/Klein

A brief summary is given on what we have learnt from inclusive DIS measurements with HERA on the structure of the proton, recalling some experimental results available twenty years ago, and presenting some HERA milestones up to most recent results.

1 Introduction

This paper summarises a seminar given at the PHOTON09 conference. It therefore is not a typical conference contribution. The seminar title was "What have we learned on proton structure from HERA?" devoted to the collider experiments H1 and ZEUS. This subject is difficult to discuss on a few proceedings pages. Before HERA, and following the seminal discovery of pointlike constitutents of the proton at SLAC, now 40 years ago, a series of neutrino and muon deep inelastic scattering (DIS) experiments was performed in order to study the partonic structure of nucleons further and to also develop and test Quantum Chromodynamics (QCD), which had been put forward as the gauge field theory of the strong interaction of confined quarks and gluons. Some of the findings of these fixed target experiments are recalled here in order to understand better the new developments which HERA brought. The kinematic range of these experiments was determined by the cms energy squared, $s = 2M_pE_l$, i.e. by the lepton beam energy E_l, typically 200 GeV, and the mass of the proton M_p as the fixed target energy.

HERA collided electrons (and positrons) of 27.5 GeV energy with protons of 820/920 GeV energy. There were three main reasons for HERA to provide a much deeper understanding of proton's structure than the fixed target experiments of the eighties: i) The energy s was much increased with the now moving proton "target", to values of $s = 4E_eE_p \simeq 10^5\,\mathrm{GeV}^2$, more than two orders of magnitude higher than before; ii) At the collider, the scattering kinematics is determined from the scattered electron angle and energy, from the hadronic final state or/and from a combination of the electron and hadron momenta. The redundancy of the kinematics was at the origin of the reliability and large kinematic range of the HERA measurements; iii) The two collider experiments H1 and ZEUS had a nearly 4π acceptance which enabled the radiative corrections to be much suppressed by establishing the energy-momentum balance of each event.

In this very brief summary a few developments may be recalled only, and the discussion is restricted to inclusive scattering. A detailed overview on experimentation at HERA and the results achieved with the data taken until 2000, in period I, can be found in these proceedings and in [1]. The slides of this talk are available from the PHOTON09 web site.

Section 2 presents a reminder on experimental results on DIS available before HERA. Section 3 recalls the first two major observations, made by H1 and ZEUS, the rise of the proton structure

function $F_2(x, Q^2)$ towards low x and the existence of a significant fraction of events, in which the proton remained intact, a process then termed deep inelastic diffractive scattering. It also reminds of ideas, discussed in 1994, on the increase of the luminosity and future measurements, in particular of the longitudinal structure function F_L, which eventually was pursued prior to the termination of HERA's operation in 2007. Section 4 presents most recent results which have allowed completing the analysis of the HERA I data, a combination of H1 and ZEUS measurements and a joint QCD analysis. Section 5 presents some recent preliminary results, based on the full HERA statistics, completion of which will end the analysis of the inclusive cross section data in the not far future. A short summary is presented in Section 6.

2 Experiments before HERA

Twenty years ago, seven major experiments on deep inelastic scattering (DIS) were analysing data, the BCDMS, BFP and EMC muon experiments and the BEBC, CCFRR, CDHSW and CHARM neutrino experiments. These experiments measured neutral (NC) and charged current (CC) scattering, respectively, at values of momentum transfer squared Q^2 up to some $100\,\mathrm{GeV}^2$ and Bjorken x values above 0.01, as is summarised in [2].

The inclusive DIS cross section, at lower Q^2, is determined by the two proton structure functions F_2 and F_L as

$$\frac{d^2\sigma}{dxdQ^2} = \frac{2\pi\alpha^2}{Q^4 x}[(Y_+ + \frac{M_p^2 x^2}{Q^2}y^2)F_2 - y^2 \cdot F_L] \simeq \frac{2\pi\alpha^2}{Q^4 x}Y_+[F_2 - \frac{y^2}{Y_+}F_L], \qquad (1)$$

where $y = Q^2/sx$ is the inelasticity of the process, or the relative energy transfer in the fixed target configuration, and $Y_+ = 1+(1-y)^2$. The structure function expression $F_2 - y^2/Y_+ \cdot F_L$ is referred to as the reduced DIS cross section σ_r. In the Quark Parton Model (QPM) for photon exchange, F_2 is determined by the sum of quark and anti-quark distributions weighted by the electric quark charges squared $F_2 = x\sum e_q^2(q + \overline{q})$, and $F_L = 0$.

Figure 1 shows one of the salient measurements of that time, the structure function $F_2(x, Q^2)$, for different x between 0.07 and 0.75 as a function of Q^2, from 9 to $220\,\mathrm{GeV}^2$, as obtained by the BCDMS Collaboration in μp scattering [3]. This data set, a combination of data from four different muon beam settings, has been crucial input for most of the subsequent extractions of parton density functions (pdf) until today. With an accuracy of up to about 2%, the data are rather precise, with good coverage of the large x region. The plot illustrates that the BCDMS data continue the behaviour of the historic SLAC ep data, obtained at lower Q^2, albeit some trend is visible of F_2 being a bit flatter at larger x in the BCDMS measurement. The tendency of the BCDMS data to be 'flat' leads to a rather small value of the strong coupling constant α_s, of about 0.11 at $Q^2 = M_Z^2$ when using the BCDMS data alone. There is also a clear deviation visible of the EMC data from the BCDMS result, in particular at lower x (left part of the plot). It was realised subsequently that the EMC analysis was incomplete at low x, and the BCDMS result was supported by the CDHSW data. The BCDMS Collaboration had also deuteron data taken, as did many other DIS fixed target experiments, unlike HERA, which was not given the time to study the structure of the neutron in the much extended range.

Using the variation of the muon beam energy, the BCDMS collaboration determined the ratio of the cross sections of longitudinally and transversely polarised virtual photon-proton interactions, $R = \sigma_L/\sigma_T = F_L/[(1 + M_p^2 x^2/Q^2)F_2 - F_L] \simeq F_L/[F_2 - F_L]$. The result, as shown in Figure 2, covers an x range from about 0.1 to 0.65 with a tendency to larger R values of

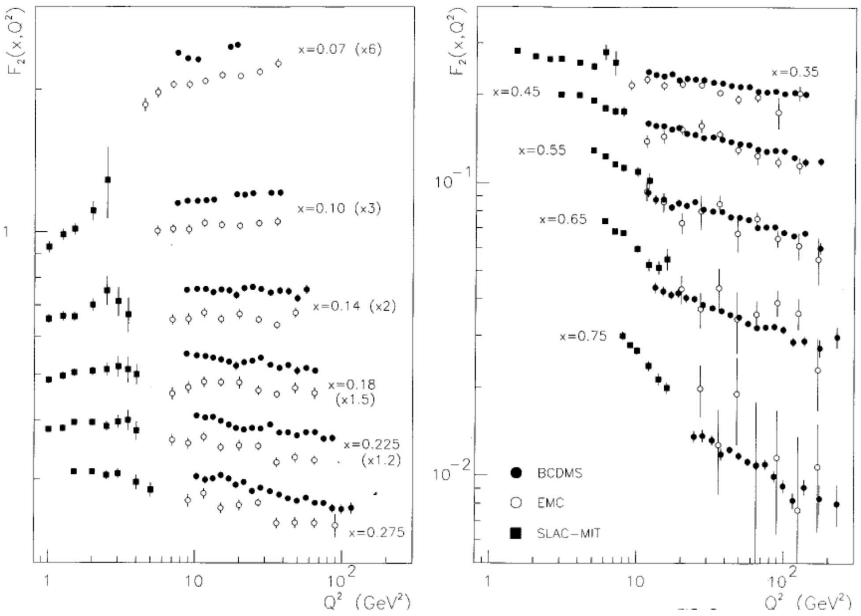

Figure 1: Solid points: Combined measurement of F_2 by BCDMS at low x (left) and large x (right). Open points: Corresponding data from EMC. Squares at lower Q^2: F_2 measured in ep scattering at SLAC.

about 0.15 towards smaller x values. Since F_L is sensitive to the gluon distribution xg [4], an increase of R may be caused by an enlarged xg. The information on xg available from the fixed target DIS experiments had yet been sparse. The gluon distribution cannot be measured directly but is deduced from QCD analyses. Since it does not enter the non-singlet evolution equations, obeyed by the valence quarks which dominate at high x, it is difficult to extract xg accurately from large x DIS data alone. An attempt to determine xg was performed by the BCDMS Collaboration [5]. Using the momentum sum rule and fixing α_s, the result of Figure 2 was obtained for a few x bins around $x \sim 0.1$. The solid overall curve describes the NLO QCD fit result [5] giving $xg = 4.93(1-x)^{8.3}$ at $Q^2 = 5\,\mathrm{GeV}^2$.

A series of DIS neutrino and anti-neutrino scattering experiments provided complementary information to the muon experiments. These experiments, by the nature of the W exchange, are sensitive to the flavour decomposition of proton structure. An example is given in Figure 3, which shows the simultaneous measurement by CDHSW [6] of the sum of the anti-quark distributions and of F_L, expressed as R, in the range of x between 0.015 and 0.65 and of Q^2 from about 0.5 to 200 GeV^2. This decomposition relies on the different y dependence, at large y, of the anti-neutrino and neutrino-nucleon scattering cross section difference on $\overline{q}$ and F_L

$$\frac{1}{\sigma_0}\left[\frac{d^2\sigma^{\overline{\nu}N}}{dxdy} - (1-y)^2\frac{d^2\sigma^{\nu N}}{dxdy}\right] = [1-(1-y)^4]\overline{q}^{\overline{\nu}} + [(1-y)-(1-y)^3]F_L. \qquad (2)$$

The result on R is very similar to the one from BCDMS. One also notices the result from the electron scattering experiment at SLAC and the strong Q^2 dependence of R at fixed, large x as shown in Figure 3. The result on the anti-quark distribution exhibits strong positive scaling

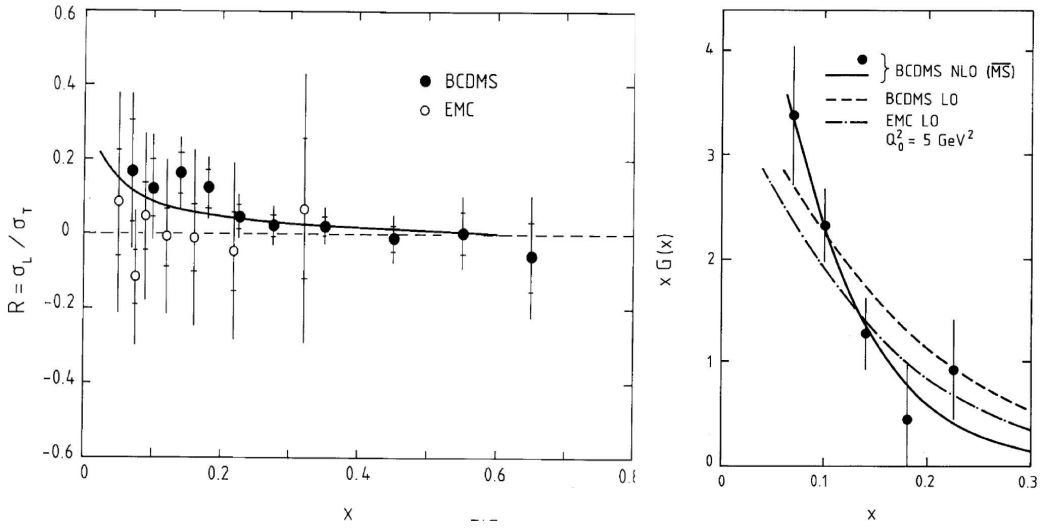

Figure 2: Measurements of $R \simeq F_L/(F_2 - F_L)$ by the muon DIS experiments BCDMS and EMC (left). Determination of the gluon distribution in NLO QCD by BCDMS (points and solid line) compared with LO determinations by BCDMS and EMC, at $Q_0^2 = 5\,\mathrm{GeV}^2$ (right).

violations at small x, down to 0.01. From the νN and $\overline{\nu} N$ cross sections it was also possible to disentangle the x behaviour of the sum of quark and anti-quark distributions, $q + \overline{q}$, and their difference, which in the QPM was assumed to be equal to the valence quarks $q - \overline{q} = u_v + d_v$. As Figure 3 illustrates, it was found that above $x \simeq 0.3$ the proton structure was dominated by valence quarks. QCD analyses showed that at low x the gluon distribution was exceeding the quark distributions.

The determination of parton distributions twenty years ago had already reached a certain state of art [7, 8]. Based on the Buras-Gaemers type of parameterisation [9], $xP \propto x^{\lambda}(1-x)^{c}$, fits were performed up to next to leading order (NLO), using global data sets, including systematic errors and renormalisation scheme effects. The predictions for HERA were of wide range, as is illustrated in Figure 4. The low x behaviour was determined by the parameter λ which was predicted to change rapidly with Q^2. The value of λ was not fixed. In an alternative approach [10], parton distributions were radiatively generated, assuming that at a very small initial scale $Q_0^2 \sim 0.3\,\mathrm{GeV}^2$ both xg and $\overline{q}$ are zero and the renormalisation group equation would still hold. This allowed predictions to be made for the behaviour of F_2 in the so far unexplored range of very small Bjorken x, down to 10^{-4}. Results from HERA were eagerly awaited.

3 First Results

The first years at HERA were particularly exciting and lead to a very large number of first observations and non-observations, as of lepto-quarks, which are reviewed in [1]. For the subject of proton structure two observations were probably of key importance, the rise of F_2 at low x

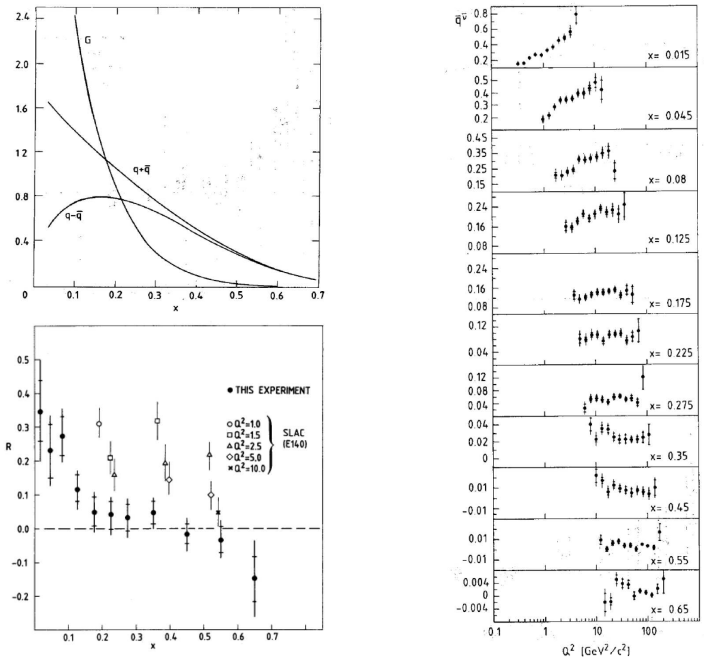

Figure 3: Right: Measurement of the total anti-quark distribution as a function of Q^2 for different x by CDHS. Left bottom: Measurement of R derived from the y distribution, compared with SLAC data at different Q^2 (open points). Left top: Determination of the sum and differences of the the total quark and total anti-quark distributions and also of the gluon distribution as a function of x, at $Q^2 = 20\,\mathrm{GeV}^2$.

and diffractive DIS.

The first measurements of the proton structure function F_2, shown in Figure 5, were based on only $0.03\,\mathrm{pb}^{-1}$ of data, taken in 1992. With these first measurements the rise of F_2 towards low x was discovered. This rise is in agreement with general expectations on the low x (large $\omega = 1/x$) asymptotic limit of QCD [11]; however, the actual scale (Q^2), at which the limit would be applicable, was not predicted. The dynamical parton model approach, termed GRV91 in Figure 5, was rather successful.

A second surprise came when an excess was observed of events with a much reduced activity in forward direction, usually populated by the remnants of the proton being in colour connection with the struck quark fragments. In 1993 an about 10% fraction of events was observed, see Figure 6, in which apparently the proton yet stayed intact. The interpretation is that of a diffractive exchange, often termed the Pomeron, which carries a fraction x_{IP} of the proton momentum. A parton of momentum fraction $\beta = x_{IP}/x$ interacts with the exchanged photon of virtual mass squared Q^2. The salient feature of these events is the absence of forward particle production, near the proton beam pipe, which is measured as an activity gap in polar angle, or equivalently rapidity, from the proton beam axis to the more centrally produced particles which stem from the struck parton in the diffractive exchange. Factorising out the Pomeron flux, the hard γIP scattering part can be treated as in conventional DIS. This allowed QCD

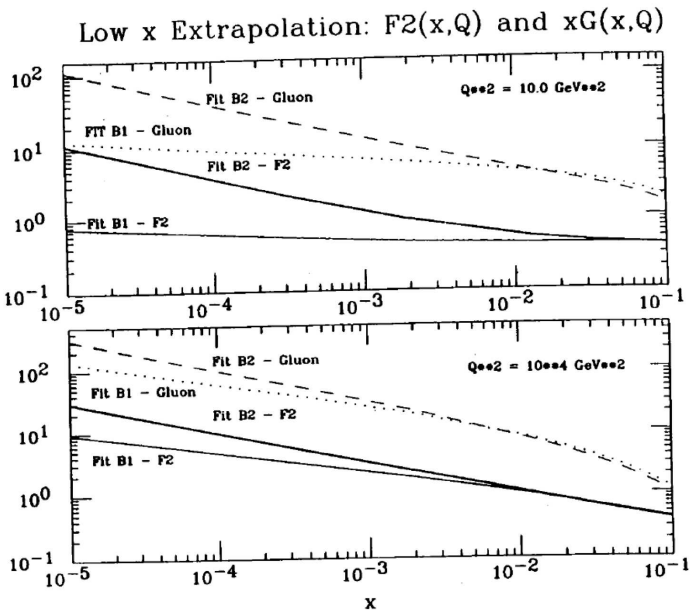

Figure 4: Extrapolation of the behaviour of F_2 and the gluon distribution xg towards low x at $Q^2 = 10$ (top) and $Q^2 = 10^4\,\mathrm{GeV}^2$ (bottom) within the framework of the 1991 global pdf analysis [7]. The low x behaviour was phenomenologically determined by the term x^B, which could be large or small. Both fits described the data which extended down to x about 0.01 at a few GeV^2. From the measurements of HERA one now knows that F_2 at $Q^2 = 10\,\mathrm{GeV}^2$ and $x = 10^{-4}$ is about 1.7 and $xg \simeq 13$, thus somewhat closer to the B_1 curves.

analyses to be performed in order to derive the quark and gluon distributions of the diffractive exchange. Such analyses are based on the diffractive cross section $\sigma^{D(3)}$

$$\frac{\mathrm{d}^3\sigma^{ep\to eXY}}{dx_{IP}dxdQ^2} = \frac{2\pi\alpha^2}{xQ^4}\cdot Y_+ \cdot [F_2^{D(3)} - \frac{y^2}{Y_+}F_L^{D(3)}], \tag{3}$$

which is integrated over the ranges of four-momentum transfer from the incoming to the outgoing proton and the dissociation mass. Similarly to inclusive DIS, the reduced ep cross section depends on the diffractive structure functions $F_2^{D(3)}$ and $F_L^{D(3)}$. For y not too close to unity, $\sigma_r^{D(3)} = F_2^{D(3)}$ holds to very good approximation. The field of diffractive DIS has developed very much as the comparison of the first observations with a recent measurement of $\sigma^{D(3)}$ illustrates, Figure 6. The major result of detailed QCD analyses has been that the diffractive interaction dynamics, or the partonic contents of the diffractive exchange, for all β below about 0.3, is dominantly due to gluons, in line with the view of the Pomeron representing a colourless exchange of two gluons.

In September 1994 a first meeting was held between the collider experiments and the HERA machine experts in order to discuss the future. The luminosity development until then was steady, as is illustrated in Figure 7, but the expectations had been on about $100\,\mathrm{pb}^{-1}$ annually while by then only about $5\,\mathrm{pb}^{-1}$ had been collected. It was obvious that for the physics at high Q^2 a much higher integrated luminosity was required. The machine was achieving an annual

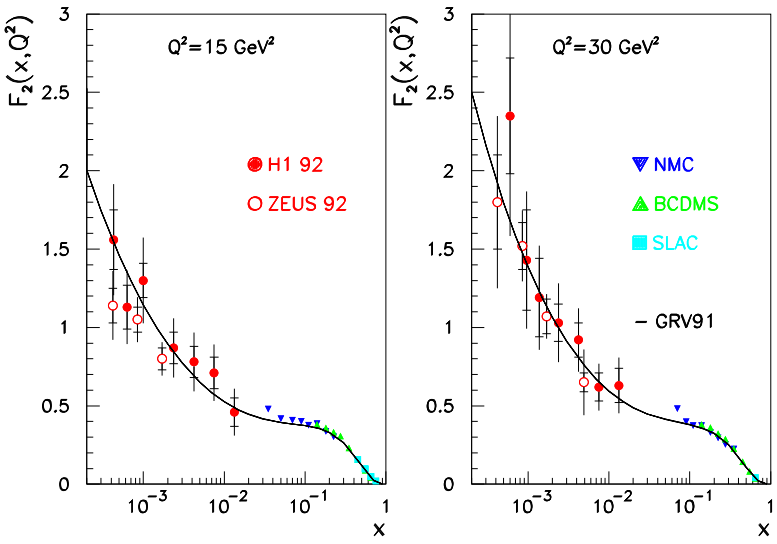

Figure 5: The first measurements of H1 (solid points) and ZEUS (open points) of the proton structure function $F_2(x, Q^2)$ based on the data taken in 1992 shown as a function of Bjorken x. The HERA experiments were able to extend the kinematic range of the F_2 data provided by the fixed target electron (SLAC) and muon (BCDMS, NMC) proton experiments by two orders of magnitude into the then-unknown domain of low x. For GRV91 see text.

luminosity close to the expectations by summer 2000 when phase I was terminated and a major upgrade began, in particular of the interaction regions. The result of placing focussing magnets close to the vertex was an increase of the specific luminosity by a factor of 4 which lead to a large increase of the luminosity when HERA had overcome initial problems due to synchrotron radiation initiated background.

At the 1994 meeting a further 'first result' was discussed. Besides a measurement of the structure functions F_2 and F_2^D there was an obvious interest in the measurement of the longitudinal structure functions, F_L and F_L^D, because these would allow a non-trivial test of QCD at higher orders and provide independent information on the gluon density at low x. Figure 8 presents the expectation on the measurement of R and the recently released, still preliminary, measurement of F_L. The result is interesting: at Q^2 lower than about 10 GeV^2, a region accessed with the upgraded backward apparatus of H1, the data tend to exceed the NLO QCD fit prediction which essentially is derived from the $\ln Q^2$ derivative of F_2. The definition of F_L to NLO and the exact treatment of the charm contribution near threshold are theoretical issues under discussion. The data analysis is being finalised to accomplish publication of this first observation [12], relying on the last data taken at HERA. Further interesting results on F_L have also been obtained by ZEUS [13] while H1 has also measured F_L^D for the first time [14].

4 Precision Results

Since the first results on F_2 in the DIS region of Q^2 of O(10) GeV^2, obtained with the initial data, the accuracy of this measurement was constantly improved. The most accurate measurement

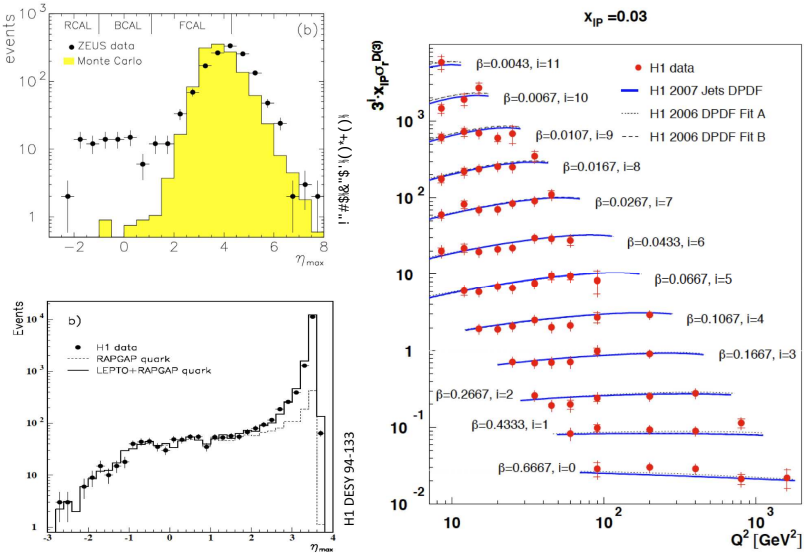

Figure 6: Left: The first observations of hard diffraction - top left: Distribution in DIS events of η_{max}, the maximum pseudorapidity of a cluster of energy larger than 400 MeV, in the ZEUS calorimeters; bottom left: Similar observation in the H1 DIS η_{max} distribution compared with a simulation which included diffractive and genuine DIS events. Right: An example for a recent measurement of the diffractive DIS cross section as a function of Q^2 for different β at $x_{IP} = 0.01$. The data are well described by a theoretical model based on QCD evolution of diffractive parton densities using a Regge factorisation ansatz.

of F_2 at HERA is shown in Figure 9 and may be compared for curiosity with Figure 5. Based on H1 detector upgrades in the mid nineties, a huge step of improvement could be realised [15] and F_2 is now known to nearly 1 % accuracy. The structure function rises approximately as x^{λ} towards low x. There is no sign of saturation of this behaviour at lowest x in the DIS region observed. Using the 1997 H1 data the power was determined [16] as $\lambda = -0.05\ln(Q^2/0.3^2)$ with Q^2 in GeV^2. Together with a variety of measurements on neutral (NC) and charged current (CC) scattering by H1 and ZEUS, a first inclusive cross section combination was recently published [17] of all HERA I data, which covers the wide kinematic range of $6 \cdot 10^{-7} \leq x \leq 0.65$ and $0.045 \leq Q^2 \leq 30000\,\text{GeV}^2$. Due to the independence of the H1 and ZEUS results and the use of complementary methods of kinematic reconstruction, the accuracy of the combined data set is better than that of a simple mean.

The combined data set was used for an updated QCD analysis at NLO [17] following the approach introduced in [15] by H1, regarding in particular the parameterisation of the parton distributions and the treatment of uncertainties. As compared to the QCD fits prior to HERA, mentioned above, quite some substantial improvements to the art of extracting parton information from DIS cross sections have been introduced over the years. These rely on experimental progress as summarised in [1] and theoretical developments, especially the challenging calculations of QCD to higher orders which reached the NNLO level [18]. These improvements are: i) a refined treatment of experimental uncertainties in terms of their uncorrelated and correlated error contributions; ii) a choice of parameters based on χ^2 saturation criteria supplemented

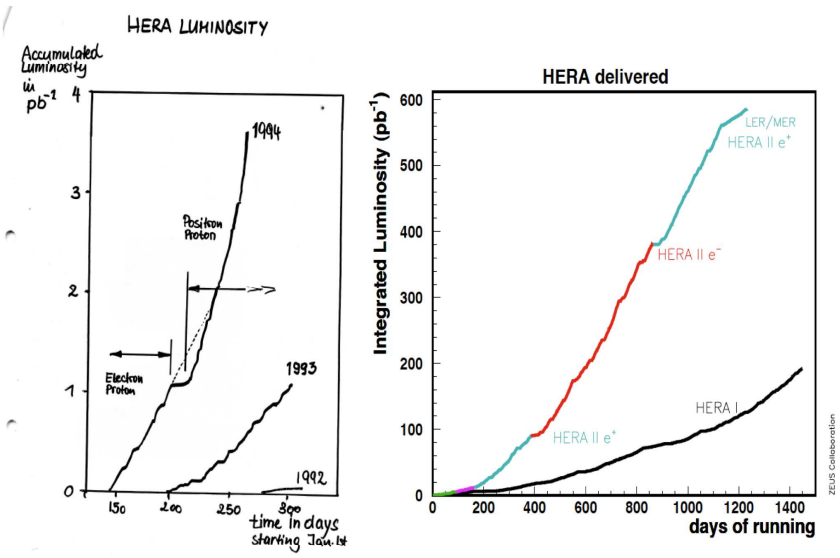

Figure 7: Development of the integrated luminosity at HERA over time. Left: Status in September 1994 as presented by Ferdinand Willeke at an upgrade meeting; right: The luminosity delivered by HERA in the first phase (1992-2000) and the upgrade phase (2003-2007). The last four months were devoted to the lower proton beam energy runs. The trend resembled HERA I as the luminosity is proportional to E_p^{-2}, i.e. the factor 3-4 loss due to the reduction of E_p at the end of HERA's operation brought the luminosity back to HERA I values of about $10^{-31}\,\mathrm{cm}^{-2}\,\mathrm{s}^{-1}$.

by in depth investigations of possible and inacceptable fit solutions; iii) attempts to consider such parameterisation uncertainties in the final error bands; iv) following the measurements of charm and beauty densities by H1 and ZEUS and theoretical prescriptions, still developing, a simulation of the threshold effects of c and b density contributions; v) a consideration of the effect of parameters such as cut or mass values. The results therefore are more reliable, not only due to the improved experimental input. There remains an element of subjectivity in performing such analyses, which underlines the importance of having several approaches, some of which are cited below [19]. There are yet some common observations associated to HERA data which may be illustrated well with the recent HERAPDF1.0 fit result [17] in Figure 10. The apparent structure of the proton depends on the resolution $\propto 1/\sqrt{Q^2}$, with which it is probed. At Q^2 of about $1\,\mathrm{GeV}^2$, corresponding to 0.2 fm, the proton structure may be decomposed as is shown in Figure 10 top. The gluon distribution has a valence like shape, i.e. at very low x the momentum is carried by sea quarks. At medium $x \sim 0.05$ the gluon dominates over all quarks. At largest x, above 0.3, the proton structure is dominated by the up and down valence quarks. This picture evolves such that below 10^{-16} m for $x \leq 0.1$ the gluon density dominates also over the sea quark density, see Figure 10 c,d). One may compare this HERA result with the early determination of xg by BCDMS, as shown in Figure 2, or the pdf determination by CDHS, Figure 3, to judge upon the immense progress achieved. The valence quarks are rather insensitive to the resolution, i.e. for any Q^2 a rather constant behaviour of the valence quarks is observed which is a feature of their non-singlet transformation behaviour in QCD.

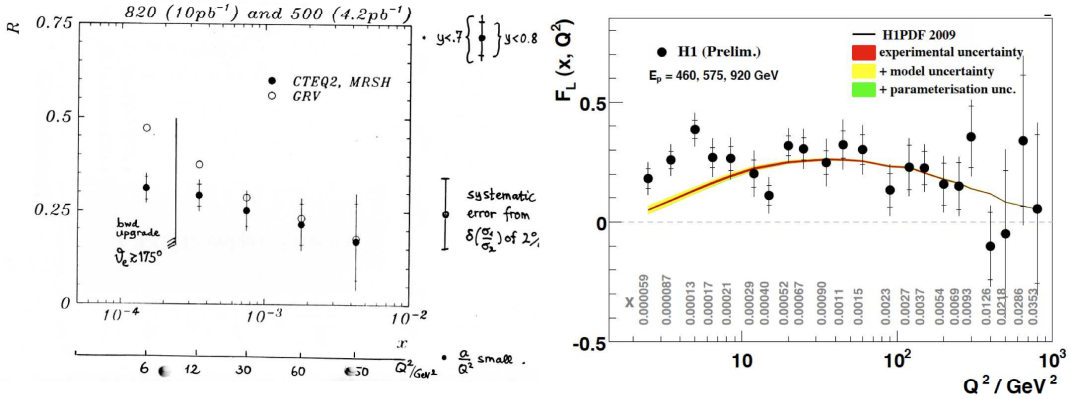

Figure 8: Left: Projected measurement of $R = F_L/(F_2 - F_L)$ as presented to the upgrade meeting in September 1994. The plot indicates the need for an upgrade of the backward region for accessing the region below Q^2 of about $10\,\mathrm{GeV}^2$. Right: Measurement of F_L with data taken 15 years later. In the low Q^2 region the predictions from various fits differ most, and the H1PDF2009 calculation tends to be below the still preliminary data.

5 Outlook

In the second phase of beam operation, HERA II, a much increased integrated luminosity was taken. For e^-p, a tenfold increase was achieved because in HERA I, due to lifetime limitations from trapped dust particles, only $15\,\mathrm{pb}^{-1}$ could be registered. Figure 12 shows the so far most accurate data on the inclusive CC scattering[1], $e^-p \to \nu X$, provided by ZEUS. One sees that the striking characteristics of CC, the missing transverse momentum, is well understood. The Figure also illustrates the confirmation of the linear dependence of the CC cross section on the lepton beam helicity. Unlike NC, the CC cross section is sensitive to the flavour contents of the proton. This is shown in Figure 12 with the decomposition of the cross section into the up quark part, $u+c$, and the down quark part $\overline{d}+\overline{s}$, weighted by $(1-y)^2$. At highest Q^2 the data extend to $x = 0.65$, albeit with limited accuracy. Currently the H1 experiment is completing a similar analysis. It then is intended to combine the H1 and ZEUS HERA II measurements, which will improve the accuracy obtained from the combination, illustrated in Figure 11, especially in the high Q^2 domain.

Deep inelastic scattering is the cleanest method to search for sub-substructure effects in the proton. The results from HERA, based on the total data statistics, limit a possible quark substructure, within the most simple form factor approach, to a dimension below $6 \cdot 10^{-19}\,\mathrm{m}$, which is about a factor of 100 below where quarks appeared and a factor of 1000 below the radius of the proton. This is deduced by both H1 and ZEUS from the Q^2 behaviour of the inclusive NC cross section. This and a number of further results are being finalised by the collaborations.

[1] A salient feature of HERA was that it measured simultaneously the NC and the CC scattering processes. Thus H1 and ZEUS were the equivalent, at much increased kinematic range, of both the charged lepton (e, μ) and the neutrino fixed target scattering experiments of the past. Loosely speaking, H1 for example was BCDMS and CDHS in one apparatus, and it also combined many physicists from these and similar experiments.

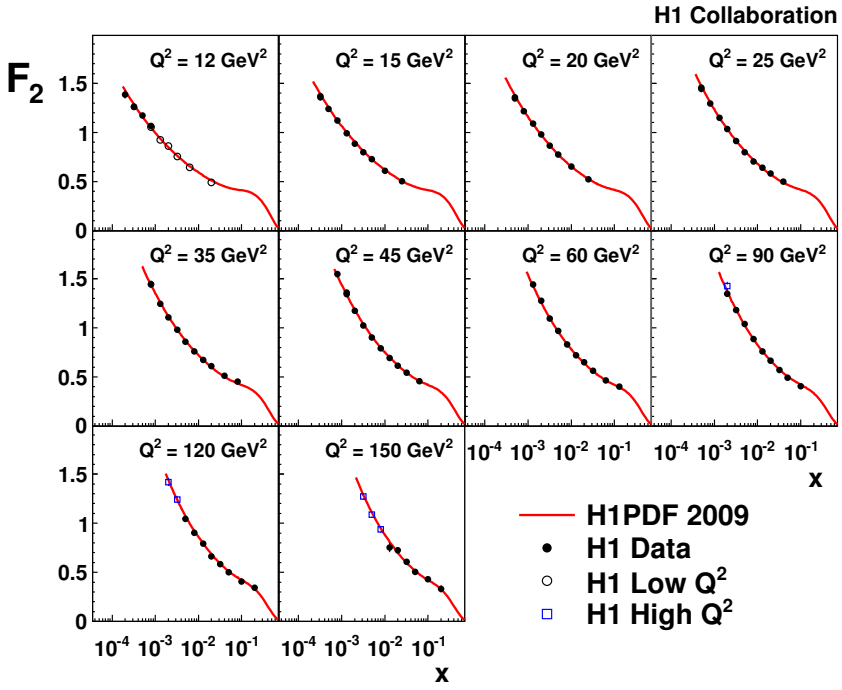

Figure 9: Recent precision measurement [15] of F_2 based on the H1 data taken in 2000.

6 Summary

So, what has been learned with HERA on the proton structure? This is not easily summarised in a few statements because H1 and ZEUS found a new world of parton dynamics inside the proton. Major observations which were not known before are: i) there is no substructure of quarks down to $6 \cdot 10^{-19}$ m; ii) the gluon momentum distribution, for $x \lesssim 0.1$, dominates the proton structure having evolved from very small values at low x and $Q^2 \simeq 1\,\mathrm{GeV}^2$; iii) QCD at higher orders is able to describe the dynamic change of partonic momentum distributions with linear evolution over more than four orders of magnitude in Q^2, with suitable parameterisations of the x dependence and question marks regarding the low Q^2, x domain as accessed with joint F_2 and F_L measurements; iv) HERA discovered diffractive DIS at the level of 10 % of the inclusive cross section. There has also been made major progress in the understanding of the hadronic final state, in the formulation of parton amplitudes from deeply virtual Compton scattering, in the measurement of the heavy quark contents of the proton including its theoretical description, and further areas of lepton-nucleon scattering not covered here.

HERA has been a major and extremely successful milestone in the development of particle physics. Ahead are still a large number of problems, some raised by HERA, to be solved for an understanding of nucleon's structure. These, for example, are: i) why are leptons and quarks different in the strong interactions; ii) is the gluon density saturating at low x, as unitarity requires, and is it equally distributed over the proton or concentrated in so-called hot spots; iii) what is the exact momentum distribution of all quarks and anti-quarks in the proton,

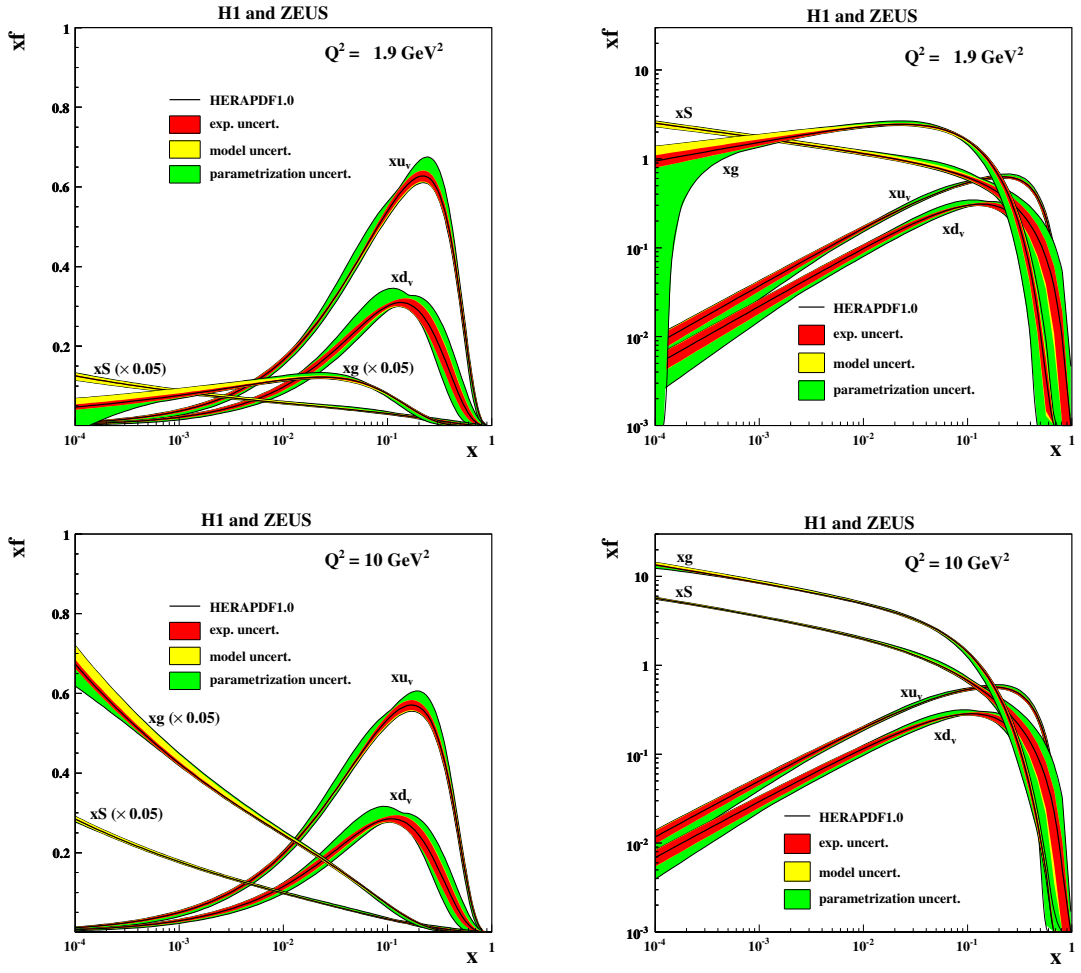

Figure 10: Parton distributions as determined by the QCD fit to the combined HERA I data at $Q^2 = 1.9$ GeV^2 (top) and at $Q^2 = 10$ GeV^2 (bottom). The inner error bands show the experimental uncertainty, the middle error bands include the theoretical model uncertainties of the fit assumptions, and the outer error band represents the total uncertainty including the parameterisation uncertainty. Here $xS = 2x(\overline{U} + \overline{D})$ denotes the total sea quark density.

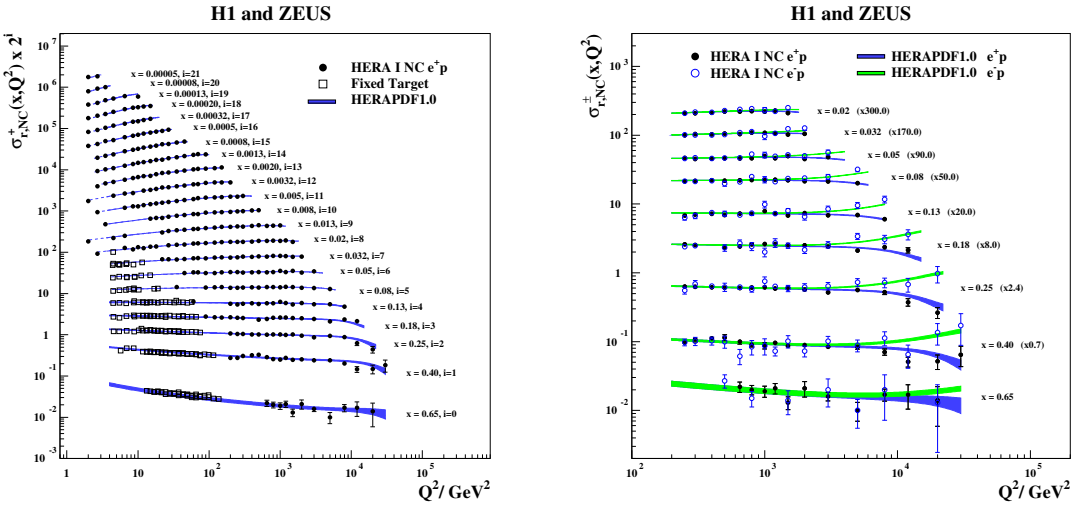

Figure 11: Combined H1-ZEUS HERA I measurement of the reduced neutral current cross section σ_r, which at lower Q^2 and y is a direct measure of the proton structure function F_2. On the right side the e^-p and e^+p cross sections are shown as open and closed symbols. The lines are from an NLO QCD fit to these data, from which at high Q^2 charge asymmetry effects are clearly visible which result from the charge dependent γZ interference cross section term.

regarding for example the strange quark density and the u/d ratio at low and at large x; iv) is there a sub-substructure at smaller dimensions than accessed by HERA; v) what is the parton dynamics and structure inside the neutron and nuclei. Searches for instantons and odderons, two peculiarities of QCD, have been unsuccessful so far. These and many further fundamental questions require a higher energy ep and eA collider to be built, which is currently under study at CERN [20] with the aim to further extend the Q^2 and x range and to increase the luminosity, both by a factor of about hundred as compared to HERA.

Acknowledgments

The invitation to this seminar turned out to be a particular event in my life for which I wish to thank Olaf Behnke, Tobias Haas and Thomas Schörner-Sadenius very warmly.

References

[1] M. Klein and R. Yoshida, Prog. Part. Nucl. Phys. **61** (2008) 343 [arXiv:0805.3334 [hep-ex]]

[2] W.-K. Tung *et al.*, Structure Functions and Parton Distributions, Fermilab Conf 89/26 (1989), Proceedings of the Snowmass Summer Study, 1988.

[3] A. Benvenuti *et al.*, BCDMS Collaboration, Phys. Lett. B **223** (1989) 485.

[4] G. Altarelli and G. Martinelli, Phys. Lett. B **76** (1978) 89.

[5] A. Benvenuti *et al.*, BCDMS Collaboration, Phys. Lett. B **223** (1989) 490.

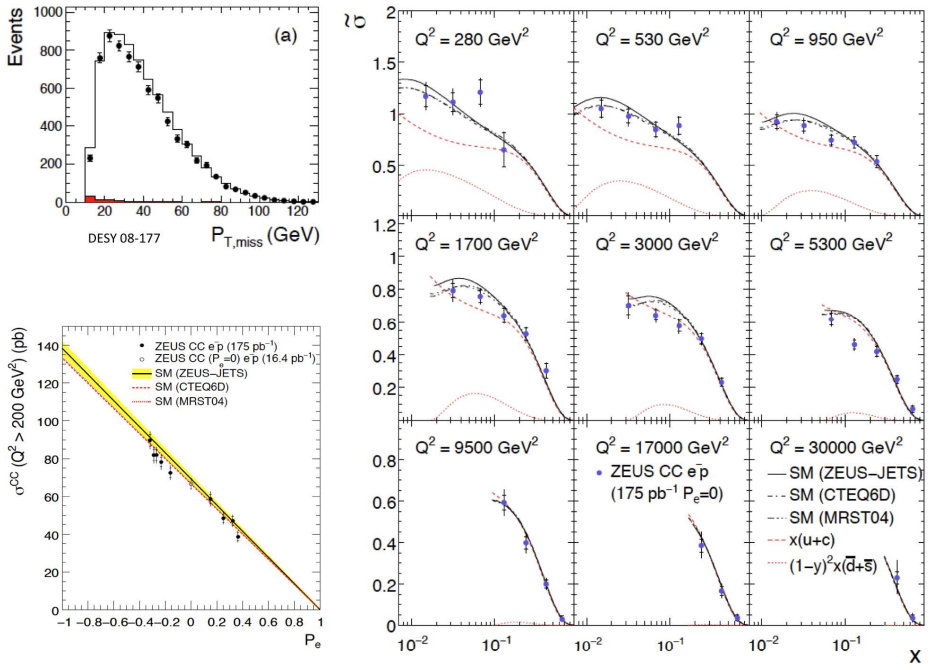

Figure 12: Measurements of CC scattering in e^-p by ZEUS. Left top: missing p_T distribution in data and simulation; left bottom: dependence of the reduced cross section on the longitudinal e^- beam polarisation; right: cross section measurement compared to various NLO QCD parameterisations.

[6] P. Berge *et al.*, CDHSW Collaboration, Z. Phys. C **49** (1991) 187.

[7] J.G. Morfin and W.K. Tung, Z. Phys. C **52** (1991) 13.

[8] P. Harriman, A.D. Martin, R.G. Roberts and W.J. Stirling, Phys. Rev. D **42** (1990) 798.

[9] A.J. Buras and K.J.F. Gaemers, Nucl. Phys. B **132** (1978) 249.

[10] M. Glück, E. Reya and A. Vogt, Z. Phys. C **48** (1990) 471.

[11] A. De Rujula et al, Phys. Rev. D **10** (1974) 1649.

[12] H1 Collaboration, Measurement of the Longitudinal Structure Function F_L of the Proton at Low x in an extended Q^2 range, H1prelim-09-044 (2009) submitted to DIS09, Madrid.

[13] S. Chekanov et al., ZEUS Collaboration, Phys. Lett. B **682** (2009) 8.

[14] H1 Collaboration, Measurement of the diffractive longitudinal structure function F_L^D, H1prelim-09-011 (2009) submitted to DIS09, Madrid.

[15] F.D. Aaron et al., H1 Collaboration, Eur. Phys. J. C **64** (2009) 56, arXiv:0904.3513 [hep-ex].

[16] C. Adloff et al., H1 Collaboration, Phys. Lett. B **520** (2001) 183 [arXiv:hep-ex/0108035].

[17] F.D. Aaron et al, H1 and ZEUS Collaborations, DESY 09-158, submitted to EPJ, arXiv:0911.0884 [hep-ex].

[18] J.A.M. Vermaseren, A. Vogt and S. Moch, Nucl. Phys. B **724** (2005) 3 [hep-ph/0504242].

[19] A.D. Martin, W.J. Stirling, R.S. Thorne and G. Watt, Eur. Phys. J. C **63** (2009) 189 [arXiv:0901.0002];
P.M. Nadolsky et al., Phys. Rev. D **78** (2008) 013004 [arXiv:0802.0007];
S. Alekhin, J. Blumlein, S. Klein and S. Moch, DESY 09-102, arXiv:0908.2766(2009).

[20] M. Klein, The LHeC Project, arXiv0908.2877, Proceedings DIS09, Madrid, 2009;
http://www.lhec/cern.ch